J Biomol NMR (2007) 39:97–105
DOI 10.1007/s10858-007-9178-2

ARTICLE

Simultaneous detection of amide and methyl correlations using a time shared NMR experiment: application to binding epitope mapping

Peter Würtz · Olli Aitio · Maarit Hellman · Perttu Permi

Received: 16 April 2007 / Accepted: 25 June 2007 / Published online: 24 August 2007

Abstract Simultaneous recording of different NMR parameters is an efficient way to reduce the overall experimental time and speed up structural studies of biological macromolecules. This can especially be beneficial in the case of fast NMR-based drug screening applications or for collecting NOE restraints, where prohibitively long data collection time may be required. We have developed a novel pulse sequence element that enables simultaneous detection of amide ^{15}N, ^{1}H and methyl ^{13}C, ^{1}H correlations. The coherence selection for the ^{15}N spins can be obtained using the gradient selected and coherence order selective coherence transfer, whereas the hypercomplex (States) method is simultaneously employed for the ^{13}C coherence selection. Experimental verification of proposed time-shared approach for simultaneous detection amide ^{15}N, ^{1}H and methyl ^{13}C, ^{1}H correlations has been carried out with three proteins, human ubiquitin, SH3 domain of human epidermal growth factor receptor pathway substrate 8-like protein (Eps8L1) and maltose binding protein complex with β-Cyclodextrin. In addition, the proposed methodology was applied for ligand binding site mapping on SH3 domain of Eps8L1, using uniformly ^{15}N and fractionally (10%) ^{13}C labeled sample. Our results show that the proposed time-shared ^{15}N/^{13}C-HSQC affords significant time saving (or improved sensitivity) in establishing ^{15}N, ^{1}H and methyl ^{13}C, ^{1}H correlations, thus making it an attractive building block for 3D and 4D dimensional applications. It is also a very efficient tool in protein ligand interaction studies even when combined with cost-effective labeling scheme with uniform ^{15}N and 10% fractional ^{13}C enrichment.

Keywords Coherence transfer · Epitope mapping · Eps8L1 · HSQC · Methyl groups · NMR spectroscopy · Proteins · Protein ligand interactions · SH3 · Time-sharing

Introduction

The concept of time-sharing between two NMR experiments, originally proposed by Sørensen (1990) and Farmer II (1991) has been shown to provide significant gains in sensitivity when applied to small molecules and biological macromolecules. In time-shared experiments, typically two different NMR parameters are jointly sampled during the indirect evolution period (Boelens et al. 1994). In principle, combining two consecutive experiments to a single NMR experiment, where two different coherences are detected simultaneously can provide time-saving up to theoretical 50%. In other words, sensitivity improvement per unit time by a theoretical factor of $\sqrt{2}$ can be obtained in comparison to two separately recorded NMR experiments. In practice, the theoretical factor is difficult to reach in macromolecules as transverse relaxation times are significantly shorter than for small molecules. Nevertheless, sensitivity gains of 30–40% (^{15}N) and 10–25% (^{13}C) has been obtained for smaller proteins using time-shared ^{15}N, ^{13}C HSQC experiment (Sattler et al. 1995). Sensitivity improvement has also been observed in experiments

Peter Würtz and Olli Aitio contributed equally.

Electronic supplementary material The online version of this article (doi:10.1007/s10858-007-9178-2) contains supplementary material, which is available to authorized users.

P. Würtz · O. Aitio · M. Hellman · P. Permi (✉)
Program in Structural Biology and Biophysics, Institute of Biotechnology/NMR Laboratory University of Helsinki, P.O. Box 65, Helsinki 00014, Finland
e-mail: Perttu.Permi@helsinki.fi

designed for measuring scalar and residual dipolar couplings in small proteins (Nolis and Parella 2007; Würtz and Permi 2007).

In this work we introduce novel building blocks for simultaneous detection of ^{15}N, ^{1}H and methyl ^{13}C, ^{1}H correlations, and compare the performance of the proposed methodology with the sensitivity-enhanced ^{15}N-HSQC experiment (Kay et al., 1992), the conventional ^{13}C-HSQC scheme (Bodenhausen and Ruben, 1980) and gradient selected, sensitivity enhanced time-shared ^{15}N, ^{13}C HSQC experiment (Sattler et al. 1995). The methodology is applied for simultaneous monitoring of ^{15}N/^{1}H and methyl ^{13}C/^{1}H chemical shift perturbations upon ligand binding on protein sample with uniform ^{15}N and fractional 10% ^{13}C labeling (Neri et al. 1989; Senn et al. 1989). Although not tested here, the methodology can be used for samples with uniform ^{15}N labeling and ^{13}C labeling of methyl groups in isoleucine (δ1 only), leucine and valine residues as proposed by Fesik and colleagues (Hajduk et al. 2000). In this labeling scheme, in contrast to the protocol devised for production of selectively protonated methyl groups in perdeuterated background (Gardner et al. 1996; Goto et al. 1999), the target protein is expressed with ^{13}C-enrichment in isoleucine (δ1 only), leucine and valine residues methyl groups only, which removes hampering ^{13}C–^{13}C scalar interaction. The proposed methodology can also be utilized as building blocks in time-shared NOESY experiments.

Materials and methods

The proposed ^{15}N/^{13}C$_m$-HSQC pulse scheme was recorded on 0.2 mM uniformly ^{15}N, fractionally 10% ^{13}C labeled sample of human ubiquitin, dissolved in 95/5% H_2O/D_2O with 10 mM potassium phosphate buffer, pH 5.8, in a sealed Wilmad 535 NMR tube at 25°C, and on 0.9 mM uniformly ^{15}N and fractionally 10% ^{13}C labeled *E. coli* maltose binding protein (MBP). All experiments were carried out on a Varian Unity INOVA 600 NMR spectrometer, equipped with a ^{15}N/^{13}C/^{1}H triple-resonance coldprobe and an actively shielded *z*-axis gradient system.

A two-dimensional ^{15}N/^{13}C$_m$-HSQC spectrum of the uniformly ^{15}N, fractionally 10% ^{13}C labeled ubiquitin was recorded with the pulse scheme shown in Fig. 1a–a′ at 25 °C. The spectrum was acquired with 4 transients per FID with 128 and 1700 complex points in t_1 and t_2, respectively. This corresponds to acquisition times of 51.2 (36.6) and 85 ms for ^{15}N (^{13}C) and ^{1}H, respectively. The ^{15}N shift-scaling factor κ was set to 0.4. The corresponding sensitivity enhanced ^{15}N-HSQC (Kay et al. 1992) and ^{13}C-HSQC (Bodenhausen and Ruben, 1980) experiments were recorded using identical parameters. The experimental time for each experiment was 20 min.

A detailed description of the cloning and purification of the SH3 domain of Eps8L1 will be published elsewhere (Aitio et al. unpublished results). Four two-dimensional ^{15}N/^{13}C$_m$-HSQC spectra for the interaction studies of SH3 domain together with its target peptide, were recorded using the pulse scheme shown in Fig. 1a–a′ at 25 °C. The initial concentration of SH3 was 0.2 mM. During the titration series, unlabeled peptide from CD3ε was added into the protein sample in 0:1, 0.2:1, 1.0:1, and 2.0:1 ratios. Each spectrum was acquired with 12 transients per FID using 128 and 1,700 complex points in t_1 and t_2, respectively. This corresponds to acquisition times of 51.2 (36.6) and 85 ms for ^{15}N (^{13}C) and ^{1}H, respectively. The ^{15}N shift scaling factor κ was 0.4. The total experimental time for each spectrum was 1 h.

All spectra were processed and analyzed using the standard VNMR 6.1C software package (Varian associates 2000).

Results and discussion

Our aim is to combine sensitivity enhanced ^{15}N-HSQC experiment with the ^{13}C-HSQC scheme optimized for methyl groups. The following conditions must then be considered in order to design optimal experiments. First, theoretical coherence transfer for both amide ^{15}N–^{1}H^{N} and methyl ^{13}C–^{1}H^{m} correlations should be maximized. Second, water flip back scheme should be applied for improved sensitivity since both amide and methyl protons resonate far from water signal. Third, phase cycling should be kept to a minimum, albeit without the cost by poor artifact suppression, for possible extension to higher dimensionality experiments or for fast screening.

Figure 1a depicts a basic scheme for two-dimensional time-shared ^{15}N/^{13}C$_m$-HSQC experiment for simultaneous detection of amide ^{15}N, ^{1}H and methyl ^{13}C, ^{1}H correlations in uniformly ^{15}N and fractionally 10% ^{13}C (Neri et al. 1989), or ^{15}N, ILV-methyl ^{13}C labeled proteins (Hajduk et al. 2000). The pulse sequence is a modification of the time-shared ^{15}N, ^{13}C HSQC schemes introduced earlier (Boelens et al. 1994; Pascal et al. 1994; Sattler et al. 1995; Uhrin et al. 2000; Xia et al. 2001, 2003; Frueh et al. 2006). We therefore emphasize on differing parts of the proposed pulse sequence. The experiment starts with concomitant INEPT transfer from ^{1}H to ^{15}N and ^{13}C spins (Boelens et al. 1994, Sattler et al. 1995) combined with the zz-filter and water selective flip-back pulse. The ensuing $(1+\kappa)*t_1$ periods are used for chemical shift labeling of ^{15}N coherence. The joint sampling of ^{13}C chemical shift frequencies takes place during the t_1 period. After the t_1 period, the following ^{13}C pulse converts the ^{13}C coherence to $2H_ZC_Z$ coherence. It is noteworthy that the scaling factor κ is

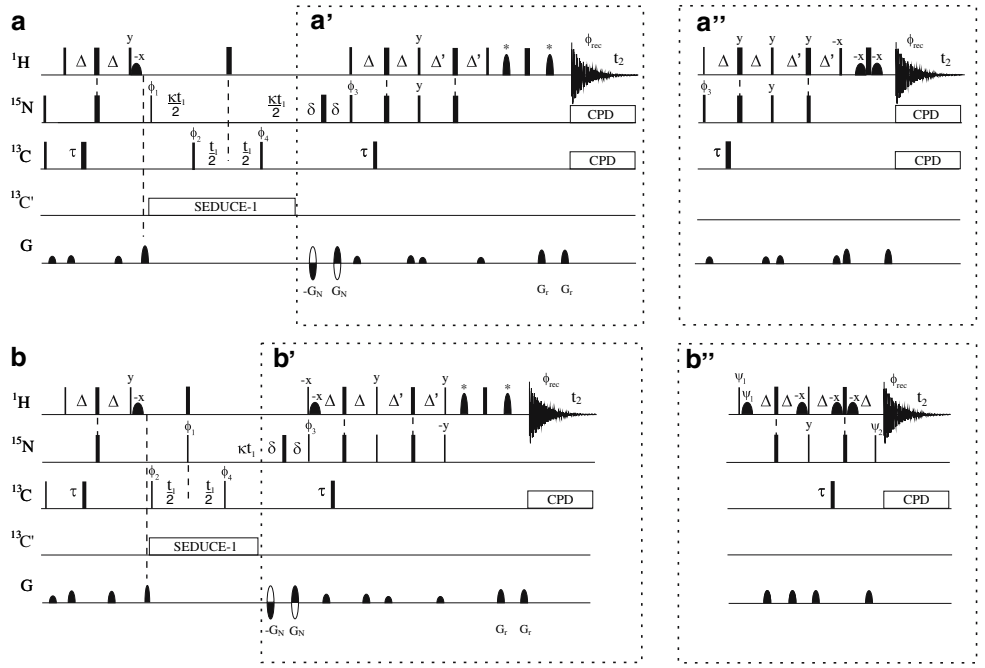

Fig. 1 Building blocks for simultaneous sensitivity-enhanced $^{15}N \rightarrow {}^{1}H$, and Cartesian antiphase $^{13}C \rightarrow {}^{1}H$ transfer and the corresponding time-shared $^{15}N/^{13}C_m$-HSQC and $^{15}N/^{13}C_m$-TROSY/HSQC experiments for simultaneous recording of ^{15}N, ^{1}H and methyl ^{13}C, ^{1}H correlations. Narrow and wide bars correspond to 90° and 180° flip angles, respectively, applied with phase x unless otherwise stated. The filled ellipsoids correspond to low power water selective flip-back pulses applied to water resonance. All 90° and 180° pulses for methyl carbons were applied with a strength of 20.8 kHz. The ^{1}H, ^{15}N, ^{13}C and $^{13}C'$ carrier positions are 4.65 (water signal), 118 (center of ^{15}N spectral region), 20 (center of ^{13}C methyl region), and 175 ppm (center of $^{13}C'$ spectral region). The methyl selective refocusing pulses (marked with asterisks) with r-SNOB (Kupče et al. 1995) or REBURP (Geen and Freeman 1991) shaping are applied off-resonance with phase modulation by Ω, where Ω indicates frequency difference between the center of methyl proton chemical shift region and water signal. (**a**) time-shared, $^{15}N/^{13}C_m$-HSQC experiment with a building block for the sensitivity enhanced $^{15}N \rightarrow {}^{1}H$, and Cartesian antiphase $^{13}C \rightarrow {}^{1}H$ transfer with (a′) or without (a″) gradient selection on ^{15}N. (**b**) The corresponding time-shared, $^{15}N/^{13}C_m$-TROSY/HSQC experiment with a building block for the sensitivity enhanced $^{15}N \rightarrow {}^{1}H$ TROSY, and Cartesian antiphase $^{13}C \rightarrow {}^{1}H$ transfer with (a′) or without (a″) gradient selection on ^{15}N. Delay durations: $\tau = 1/(4J_{CmHm}) \sim 2.0$ ms; $\Delta \sim \Delta' \sim 1/(4J_{NH}) \sim 2.0$–2.6 ms; δ = gradient + field recovery delay; $\kappa = sw_C/sw_N - 1$ for a and $\kappa = sw_C/sw_N - 1/2$ for b. Frequency discrimination in F_1 for ^{13}C in all sequences is obtained using States-TPPI protocol (Marion et al. 1989) applied to ϕ_2 In a+a′ and b+b′, the frequency discrimination in F_1 for ^{15}N is obtained using sensitivity-enhanced gradient selection (Kay et al. 1992). The echo and antiecho signals in F_1 dimension are collected separately by inverting the sign of the G_N gradient pulses together with the inversion of ϕ_3 Phase settings: $\phi_1 = x$ (y for b + b′); $\phi_2 = x, -x$; $\phi_3 = x$; $\phi_4 = x$. In a+a″, the frequency discrimination in F_1 for ^{15}N is obtained using States-TPPI protocol applied to ϕ_1. In addition, for each t_1 increment the phase ϕ_3 is inverted. Phase settings: $\phi_1 = x, -x$; $\phi_2 = x, -x$; $\phi_3 = x$; $\phi_4 = x$. In b + b″, the frequency discrimination in F_1 for ^{15}N is obtained using States-TPPI protocol (Marion et al. 1989) applied to ϕ_1. In addition, for each t_1 increment ψ_1 and ψ_2 are inverted. Phase cycling: $\phi_1 = y, -y$; $\phi_2 = x, -x$; $\phi_4 = x$; $\psi_1 = -y, y$; $\psi_2 = -x, x$. Gradient durations (strengths): $G_N = 0.55$ ms (16.5 G/cm), $G_r = 0.2$ ms (4.6 G/cm). If the individual editing of ^{13}C and ^{15}N resonances is desired, additional phase cycling (x, $-x$) can be added to ϕ_2 The adiabatic WURST-2 (Kupče and Wagner 1995) and GARP-1 (Shaka et al. 1985) decoupling sequences with field strength respectively 5.3 and 1.1 kHz were used to decouple ^{13}C and ^{15}N during acquisition. Varian pulse programs for the proposed pulse sequences are available online at http://www.biocenter.helsinki.fi/bi/nmr

defined by sw_C/sw_N–1, where sw_C and sw_N correspond to spectral widths of methyl carbon and nitrogen. As the difference between the spectral widths of ^{15}N and methyl carbons is rather small, ^{15}N and ^{13}C spectral widths can even be set equal. Thus, the sensitivity loss for methyl groups by relaxation of the longitudinal two spin order ($2H_ZC_Z$) during the κt_1 period remains low.

The pulse scheme design offers sensitivity enhancement for the amide ^{15}N–^{1}H correlations (the IS spin system) by utilizing coherence order selective coherence transfer, and retains high sensitivity for methyl ^{13}C, ^{1}H correlations (I_3S spin system) by employing conventional Cartesian antiphase transfer. This approach circumvents inherent sensitivity loss for methyl groups by a factor of 0.88 compared to gradient selection or coherence order selective coherence transfer schemes (Scleucher et al. 1994). The optimum sensitivity can be achieved either with the gradient selection for ^{15}N or without the gradients, using the *preservation of equivalent pathways* (PEP) scheme by Rance and co-workers (Palmer et al. 1991). The following back transfer step differs between the gradient selected implementation and the original PEP scheme, and hence in the following paragraphs both version are described in detail. Let us first emphasize on the gradient selected

HSQC implementation. The corresponding back transfer element is shown in Fig. 1a′. In this case, the pulsed field gradients are employed for the selection of ^{15}N coherence during the $(1+\kappa)*t_1$ i.e., two gradients with opposite polarity are applied during 2δ in order to select either echo or antiecho pathways for the ^{15}N coherence. Subsequent 90° pulses on ^{1}H and ^{15}N convert the desired magnetization to ^{1}H single-quantum coherence which is antiphase with respect to ^{15}N and ^{13}C, described by the density operators $2H_y^N N_z$ and $2H_y^m C_z$, respectively. In addition, part of the magnetization is converted into $2H_y^N N_x$ multiple-quantum coherence as in the sensitivity-enhanced ^{15}N-HSQC experiment (Kay et al. 1992). During the ensuing delays 2Δ and 2τ, the antiphase terms refocus and will be transformed to longitudinal H_Z^N and H_Z^m magnetization by the following 90° ^{1}H pulse. The multiple-quantum term is converted to antiphase $2H_y^N N_z$coherence, which refocus to H_x^N coherence during the last $2\Delta'$ delay. The final 90° ^{1}H pulse converts longitudinal components of magnetization into H_y^N and H_x^N, and H_y^m coherences. As the magnetization originating from the amide proton has been dephased by the coherence selective gradients during the indirect evolution period, whereas the magnetization originating from methyl proton has not, we have to rephase the amide proton magnetization without dephasing the methyl proton magnetization prior to acquisition. To this end, we propose the following refocusing scheme during the final spin-echo; a pair of refocusing gradients with the same polarity is applied together with two selective 180° methyl pulses (indicated by asterisk in Fig. 1a) and a hard 180° ^{1}H pulse. Two gradients with same polarity are flanking the final selective 180° methyl pulse, whereas each gradient pair with the same polarity but unequal strength are flanking the non-selective 180° ^{1}H pulse. Hence, the amide proton magnetization is rephased by the refocusing gradient as in the gradient selected, sensitivity enhanced ^{15}N-HSQC experiment. Methyl protons, or more generally those protons that are refocused by the 180° selective pulses are not affected by the gradients. In this way, it is possible to utilize the gradients for the coherence selection of the amide ^{15}N, ^{1}H correlations and simultaneously obtain the coherence selection of the methyl ^{13}C, ^{1}H correlations using the conventional hypercomplex (States) method. In addition, the pulse sequence obtains water flip-back in a manner identical to the conventional gradient selected, sensitivity enhanced ^{15}N-HSQC experiment if care is taken that water magnetization is not perturbed by the two selective 180° pulses. It is worth mentioning that owing to the difference between the phase-modulated ^{15}N/^{1}H signal obtained using sensitivity-enhanced echo/antiecho selection, and the amplitude-modulated ^{13}C/^{1}H signal in F_1, the quadrature and purely absorptive lineshape cannot be obtained simultaneously for both amide ^{15}N, ^{1}H and methyl ^{13}C, ^{1}H correlations. Thus, separate data processing is required by using the sensitivity-enhanced and hypercomplex (States) procedure for ^{15}N/^{1}H and ^{13}C/^{1}H data, respectively. As proposed originally by Sørensen (1990), ^{15}N and ^{13}C bound protons can be separated by adding additional phase cycling step (0°, 180°) to ϕ_2 pulse (Farmer II and Mueller 1994). When acquired in an interleaved manner, two data sets are generated with the sign inversion for the methyl resonances (^{15}N ± ^{13}C). Then by appropriate combination of separate data sets provides either amide ^{15}N, ^{1}H or methyl ^{13}C, ^{1}H correlations (see caption to Fig. 1 for details).

The back transfer scheme for the sensitivity-enhanced implementation without the gradient selection is shown in Fig. 1a′′. In addition to absence of coherence selection gradients, the pulse scheme differs from the gradient selected version in its water magnetization handling. In addition, four-step phase cycling is required for ^{15}N coherence selection and quadrature detection. To this end, two-step phase cycling is applied to ϕ_1 and ϕ_3 in order to remove imbalance between single- and multiple-quantum coherence transfer pathways (Palmer et al. 1991). To assure efficient water suppression with water flip-back (Grzesiek and Bax 1993) prior to acquisition period, additional spin-echo period with the WATERGATE pulse element (Piotto et al. 1992) is incorporated into the pulse sequence.

The corresponding ^{15}N/^{13}C$_m$-TROSY/HSQC versions of the experiment are displayed in Fig. 1b. A few modifications with respect to the HSQC version have to be made in order to select the most slowly relaxing ^{15}N–^{1}H multiplet component simultaneously with the methyl HSQC. Recently, an elegant 3D/4D time-shared NOESY experiment with the gradient selected TROSY and HSQC implementation for the amide ^{15}N–^{1}H and methyl ^{13}C–^{1}H moieties was introduced (Frueh et al. 2006). We prefer using a slightly different approach in order to keep the relaxation losses for ^{15}N–^{1}H moieties to a minimum and to retain coherence transfer efficiency in the level of Cartesian antiphase transfer for the CH_3 moieties for retaining the highest sensitivity. The initial part of the ^{15}N/^{13}C$_m$-TROSY/HSQC scheme is identical to the HSQC version in Fig. 1a. However, for the TROSY version the ^{13}C chemical shift labeling takes place prior to ^{15}N chemical shift incrementation. Moreover, the ^{15}N chemical-shift labeling starts after the first $t_{1/2}$ period. This can be justified by the following reasons. First, we aim for refocusing of ^{13}C–^{1}H scalar interaction during t_1 without methyl selective pulses and without compromising the TROSY effect by mixing the amide proton spin-states during ^{15}N chemical shift labeling. Although ^{15}N–^{1}H magnetization is in the form of longitudinal two-spin order $2H_z^N N_z$ for a time period equal to $t_{1/2}$, we can still use the additional $t_{1/2}$ period for

incrementation of ^{15}N chemical shift, that is, the scaling factor κ in this case is defined by $\kappa = sw_C/sw_N - 1/2$. Analogously to ^{15}N–^{1}H moieties, the methyl ^{13}C–^{1}H relaxation can be reduced by shortening the time period during which the spin system is in the form of longitudinal two-spin order $(2H_z^m C_z)$. As in the corresponding HSQC version of the experiment, two different implementations of the ^{15}N/^{13}C$_m$-TROSY/HSQC scheme, with and without the ^{15}N coherence selection using the pulsed field gradients, can be conveyed. Let us first emphasize on the implementation utilizing pulsed field gradients for the ^{15}N coherence selection (Fig. 1b′). After the ^{15}N chemical shift labeling, a pair of gradients with opposite polarity is employed for coherence selection in indirectly detected dimension. This is followed by the TROSY scheme originally suggested by Yang and Kay (1999) and later modified by Nietlispach (2005) in order to suppress the antiTROSY component. This represents optimal transfer scheme for both ^{15}N–^{1}H TROSY transition as well as for methyl ^{13}C-^{1}H correlations. The spin-state selective polarization transfer from slowly relaxing ^{15}N transition to slowly relaxing ^{1}H transition is thoroughly discussed in the original papers (Yang and Kay 1999; Nietlispach, 2005). Instead, we focus on fate of the density operator corresponding to ^{13}C –> ^{1}H transfer in methyl groups. As in the corresponding HSQC version (Fig. 1a), the 90° (^{1}H) pulse following the delay 2δ transforms the $2H_z^m C_z$ operator to $2H_y^m C_z$, which refocus during the ensuing delay 2τ. The subsequent 90° (^{1}H) pulse converts H_x^m coherence to slowly relaxing H_z^m magnetization. Again, the final non-selective 90° (^{1}H) pulse creates H_x^m coherence, which will be detected during acquisition as it bypasses the last four gradients analogously to the corresponding HSQC scheme in Fig. 1a.

The corresponding time-shared ^{15}N/^{13}C$_m$-TROSY-HSQC scheme with Single Transition To Single Transition Polarization transfer (ST2-PT) element (Pervushin et al. 1997, Andersson et al. 1998) is depicted in Fig. 1b″. The ^{15}N–^{1}H TROSY selection is established as in the generalized TROSY scheme (Andersson et al. 1998) and will not be discussed in detail. However, in order to combine the generalized TROSY scheme with the methyl selective coherence transfer without using the methyl selective pulses, a slightly different refocusing scheme is employed. Emphasizing on the fate of the $2H_z^m C_z$ density operator after t_1 period, it can be realized that the 90° (^{1}H) pulse with phase ψ_1 creates the antiphase coherence $2H_y^m C_z$, which will be solely susceptible to methyl ^{1}H spin relaxation as no 180° (^{13}C) pulse is applied during the ensuing 2Δ delay. The antiphase coherence refocuses during the delay 2τ, which is incorporated into the following ^{15}N–^{1}H spin-state selective filter with the pair of shaped pulses for the WATERGATE solvent suppression scheme. Although the overall duration of the pulse sequence utilizing the ST2-PT scheme for the TROSY selection (Fig. 1b″) is the shortest, the methyl proton magnetization remains in the transverse plane for ~2 ms longer than in the sequences in Fig. 1b′. We thus prefer using the scheme in Fig. 1b′ for the simultaneous ^{15}N-TROSY, ^{13}C-HSQC selection. Moreover, additional two-step phase cycle is required for the TROSY selection in Fig. 1b″, which somewhat limits the applicability of scheme as a general building block for multidimensional experiments.

Experimental verification of the proposed pulse schemes were carried out using three proteins, human ubiquitin, the Src homology domain (SH3) of human epidermal growth factor receptor pathway substrate 8-like protein, Eps8L1 (supplementary material), and the maltose binding protein (MBP) in complex with β-cyclodextrin (supplementary material). The SH3 domain and ubiquitin represent small ~8 kDa proteins, with good chemical shift dispersion and small transverse relaxation rates, whereas MBP/β-cyclodextrin, having a molecular mass of 42 kDa, embodies a high molecular weight protein with broad lines and significant resonance overlap. In addition, SH3 binding with its target peptide was studied by titrating target peptide into the protein sample in a stepwise manner and monitoring perturbations in both amide ^{15}N/^{1}H and methyl ^{13}C/^{1}H chemical shifts in SH3 domain by recording a time-shared ^{15}N/^{13}C$_m$-HSQC experiment at each titration point.

In order to estimate attainable sensitivity enhancement on smaller proteins, we measured the proposed time-shared ^{15}N/^{13}C$_m$-HSQC spectra on ubiquitin and compared the determined signal-to-noise ratios with the corresponding ^{15}N-HSQC and ^{13}C-HSQC spectra measured using the gradient selected and sensitivity-enhanced ^{15}N-HSQC and conventional ^{13}C-HSQC experiments. Theoretical sensitivity enhancement using a time-shared ^{15}N/^{13}C$_m$-HSQC over two consecutive ^{15}N- and ^{13}C-HSQC experiments is $\sqrt{2}$ as methyl and amide proton correlations can be established simultaneously i.e., per unit time two times more scans can be invested in a time-shared ^{15}N/^{13}C$_m$-HSQC. On smaller proteins this can be reached for the vast majority of amide ^{15}N, ^{1}H correlations since from the ^{1}H^{N} transverse relaxation point of view, the proposed pulse scheme in Fig. 1a is approximately only 2 ms longer than the gradient selected and sensitivity-enhanced ^{15}N-HSQC due to the applied selective methyl pulses. Assuming a $T_{2,HN}$ of 40 ms, the expected sensitivity loss will be less than 5%. Figure 2 shows excerpts from 1D traces along ^{1}H axis of ^{15}N/^{13}C$_m$-HSQC and ^{15}N-HSQC spectra of human ubiquitin. Both spectra were recorded using 8 transients yielding nearly identical experimental time, i.e. 10 min. The experimental results are in close agreement with theoretical considerations in ubiquitin as appreciated for K6, T7, R54 and E64 residues shown in Fig. 2. The attainable

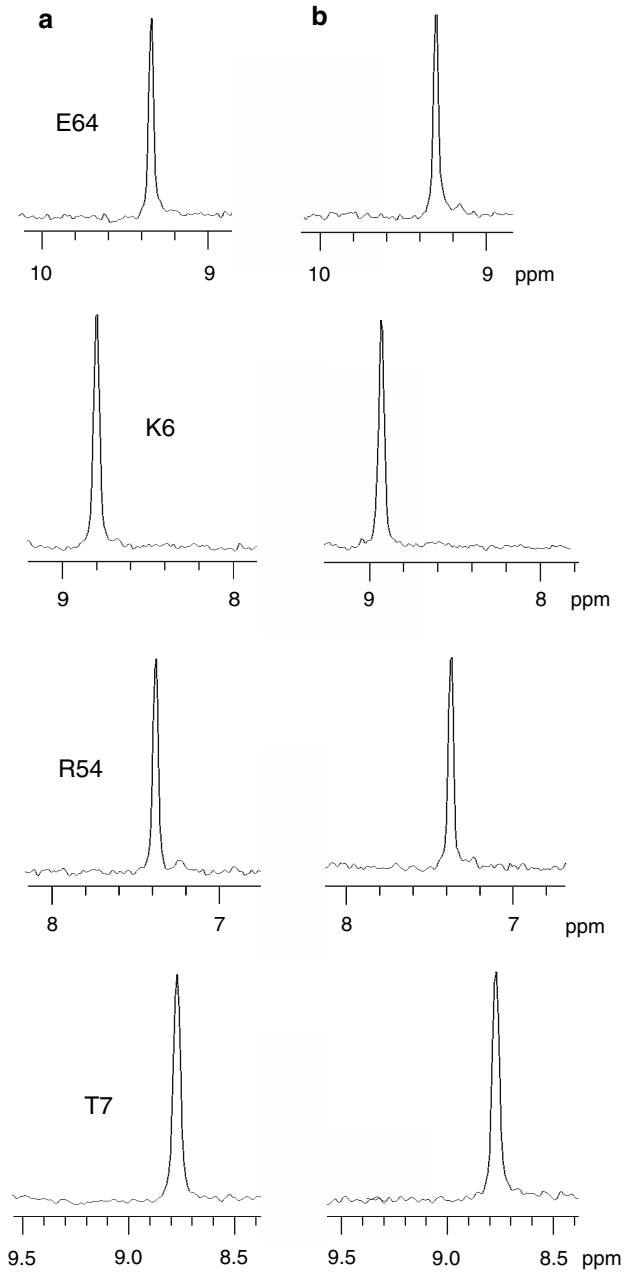

Fig. 2 Comparison of representative $F_2(^1H)$ traces of four amide ^{15}N, ^1H correlations in human ubiquitin recorded at 600 MHz using (**a**) the time-shared $^{15}N/^{13}C_m$-HSQC pulse sequence of Fig. 1a–a′, and (**b**) sensitivity-enhanced ^{15}N-HSQC experiment (Kay et al. 1992). The spectra were scaled to have identical noise floor so that the attainable sensitivity is directly comparable

sensitivities between $^{15}N/^{13}C_m$-HSQC and the conventional ^{15}N-HSQC do not deviate more than ±5%.

In case of methyl ^{13}C–^1H correlations, a small sensitivity loss in comparison to the conventional ^{13}C-HSQC experiment is inevitable if an equal number of scans are used for both experiments. This can be understood by realizing that the time-shared experiment in Fig. 1a is approximately 9–10 ms (gradient refocusing delay $+4(\Delta-\tau)+2\Delta'$) longer than the corresponding ^{13}C-HSQC experiment. This is due to the fact that in addition to the gradient refocusing delay, each concatenated INEPT step is ca. 1.5 ms longer than in the conventional ^{13}C-HSQC, assuming $^1J_{NH}/^1J_{CH}m \sim 90/123$ Hz. However, it should be noted that in the schemes of Fig. 1a–a″ and b–b′, the methyl proton magnetization is in slowly relaxing H_z^m state during the final INEPT step ($2\Delta' \sim$ 4–5.3 ms), which minimizes the sensitivity loss i.e., the methyl proton magnetization is susceptible to T_2 relaxation for ~3–5 ms longer than in the conventional ^{13}C-HSQC experiment. This leads to sensitivity loss by 10–15%, assuming $T_{2,\,H}m \sim 30$ ms. However, as two times more scans per unit time can be invested in a time-shared $^{15}N/^{13}C$-HSQC experiment, the overall sensitivity will be increased. We recorded the proposed time-shared $^{15}N/^{13}C_m$-HSQC and the conventional ^{13}C-HSQC experiments on 0.2 mM human ubiquitin with an equal number of transients, yielding virtually identical experimental time. It is noteworthy that the protein concentration is only 20 μM with respect to the ^{13}C isotope as fractional (10%) ^{13}C enrichment was employed. Indeed, a small sensitivity loss (5–10%) was observed as can be seen in Fig. 3, where 1D traces along ^1H axis are shown for several methyl correlations. This loss is also partly governed by the relaxation of $2H_z^mC_z$coherence during κt_1 period as ^{13}C spectral width was set 1.4 times larger than ^{15}N spectral width. Nevertheless, as demonstrated even for the much larger maltose binding protein, a gain in attainable sensitivity can be obtained as the number of scans can be doubled per unit time using the time-shared approach (supplementary material).

We also compared the performance of the proposed $^{15}N/^{13}C_m$-HSQC experiment against the time-shared $^{15}N/^{13}C$-HSQC experiment by Griesinger and co-workers (Sattler et al., 1995) and the well-established gradient selected, sensitivity-enhanced ^{13}C-HSQC with small ^{15}N, ^{13}C (10%) labeled SH3 domain of Eps8L1 (see supplementary material).

We employed the proposed time-shared $^{15}N/^{13}C_m$-HSQC experiment (Fig. 1a+a′) for mapping the protein-ligand binding interface of the SH3 of human Eps8L1 with its target peptide. Relatively dilute protein concentration, ~0.2 mM, of uniformly ^{15}N and fractionally ^{13}C labeled Eps8L1-SH3 was used. Thus, with respect to methyl ^{13}C labeling (~10%) the sample concentration was ~20 μM. The $^{15}N/^{13}C_m$-HSQC experiment was recorded at each titration point i.e., after addition of target peptide into the protein sample (Fig. 4). It can be readily appreciated that addition of the ligand induces significant perturbations in ^{15}N, ^1H chemical shift but also in the ^{13}C, ^1H methyl correlations for several residues. The observed perturbations in the chemical shifts of ^{15}N, ^1H and methyl ^{13}C, ^1H

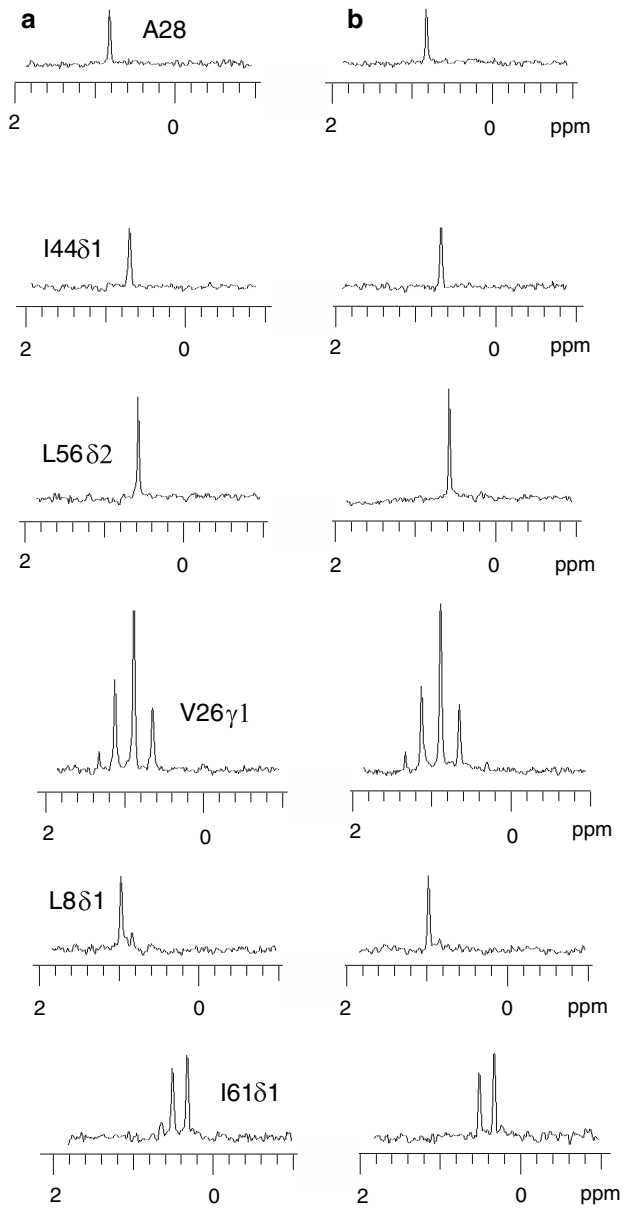

Fig. 3 Comparison of representative $F_2(^1H)$ traces of through methyl ^{13}C, ^1H correlations in human ubiquitin recorded at 600 MHz using (**a**) the time-shared $^{15}N/^{13}C_m$-HSQC pulse sequence of Fig. 1a–a′, and (**b**) conventional ^{13}C-HSQC experiment (Bodenhausen and Ruben 1980). The spectra were scaled to have identical noise floor so that the attainable sensitivity is directly comparable. The corresponding resonances are indicated with assignments

correlations demonstrates that the target peptide is tightly binding to the canonical binding site of the SH3 domain (Aitio et al. unpublished results).

Although the sensitivity of methyl correlations on such a dilute sample is excellent for binding epitope mapping, there are some additional aspects that require further consideration in comparison to the labeling scheme proposed by Hajduk et al (2000). First, homonuclear ^{13}C–^{13}C couplings decrease the sensitivity and resolution for Val $\gamma1$, Leu $\delta1$, Ile, Thr and Ala methyl groups. Second, in the labeling strategy proposed by Hajduk et al., the spectral crowding will be less serious as methyl groups of Ala, Met, Thr and Ile $\gamma2$ are absent. Third, the isotopic abundance of ^{13}C is approx. 9–10 fold smaller with respect to ligand. The first issue can be partly addressed, although not attempted here, by decoupling of Thr $^{13}C\beta$ and Ala $^{13}C\alpha$ resonances during the t_1 period in order to enhance sensitivity and resolution of the methyl groups of these residues. Furthermore, the methyl groups of Ala, Met, Thr and Ile $\gamma2$ are important structural probes. This is demonstrated for A17 and I57 in Fig. 4b′–b″, which provide a complementary view for chemical shift perturbations observed for NH of R18 (Fig. 4a′). On the other hand, methyl ^{13}C, ^1H correlation map can be used for determining the binding epitope of the ligand simultaneously. By using an excess of ligand the emergence of signals originating from the ligand can be observed. In Fig. 4b, the signal, indicated with an arrow, stems from the methyl group of a C-terminal Ile residue of the peptide ligand. Intensity of this methyl signal increases as a function of increasing peptide concentration with no significant chemical shift perturbation or line broadening, which indicates that it is not located within the binding epitope. On the other hand, the methyl signals of an N-terminal Val, located in the binding interface, become detectable as broadened resonances only, when a larger excess of peptide (5:1) is used (data not shown).

It has been shown earlier that stereo-specific assignment of diastereotopic methyl groups is of utmost importance in structure calculations. Stereo-specific assignment of methyl groups in leucine and valine residues can be obtained using biosynthetically 10% ^{13}C labeled sample (Neri et al. 1989; Senn et al. 1989). Owing to different metabolic pathways in *E. coli* the $\gamma1$ methyl groups of valine and $\delta1$ methyl groups of leucine exhibit ^{13}C–^{13}C scalar couplings whereas the $\gamma2$ and $\delta2$ do not, respectively (Neri et al. 1989). Figure 4 demonstrates that in case of small proteins such as SH3, the stereo-specific assignment of methyl groups in Leu and Val residues can readily be made using the same relatively dilute protein sample. Thus, uniform ^{15}N and fractional 10% ^{13}C labeling scheme can be utilized for protein ligand interaction studies, stereo-specific assignment of prochiral methyl groups, and also for the backbone assignment as recently proposed by Iwai and Fiaux (2007). The approach is especially attractive in single case studies where the ^{15}N labeling procedure already exists, thus no additional steps in sample preparation are required. As the preparation of fractionally 10% ^{13}C labeled sample is also cost-effective, we reckon that this kind of sample can efficiently be used for screening protein ligand interactions by observing chemical shift perturbations simultaneously on amide ^{15}N, ^1H and methyl ^{13}C, ^1H correlations.

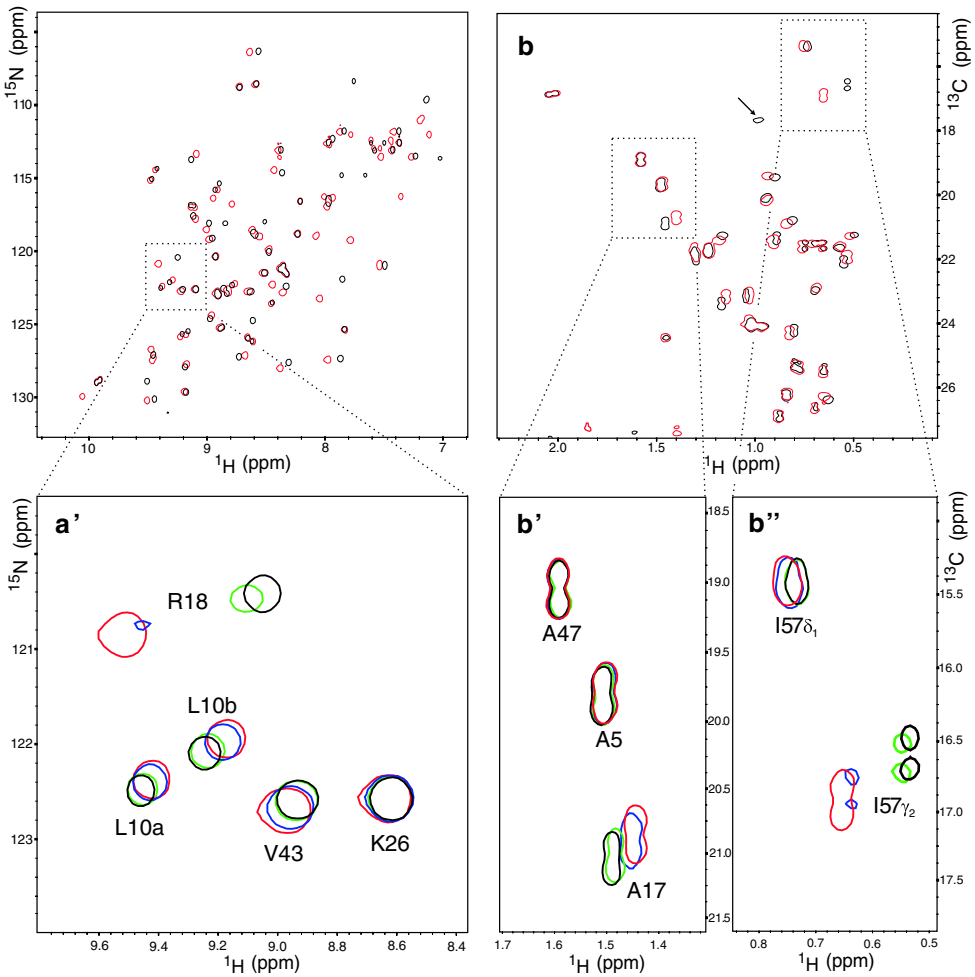

Fig. 4 ^{15}N, ^{1}H (**a**) and methyl ^{13}C, ^{1}H (**b**) correlation maps of SH3 domain free in solution (red color) and in 1:2 SH3:peptide (complex with the target peptide) (black color). Representative expansions from amide (a′) and methyl (b′ and b″) regions of SH3 show chemical shift perturbations as a function of increasing peptide concentration, the spectra recorded at each titration point are color coded and shown overlaid; 1:0 (red), 1:0.2 (blue), 1:1 (green) and 1:2 (black). Assignments for cross peaks shown in expansions are indicated. The two signals for L10 arise from the two conformers present in the SH3 domain in both free and bound form. An arrowhead points to the methyl resonance originating from the ligand in 2:1 ratio

In case of larger proteins such as MBP, sensitivity losses due to rapid spin relaxation will become more pronounced and consequently the attainable sensitivity gain becomes smaller than the theoretical 1.41 (See supplementary material). The sensitivity gain close to the theoretical maximum in ^{15}N, ^{1}H correlations can be reached for some residues although for the great majority of the correlations sensitivity gain is $\sim$15–25%. The sensitivity gain becomes smaller for methyl ^{13}C, ^{1}H correlation as faster transverse relaxation becomes more costly due longer pulse sequence with respect to the ^{13}C-HSQC. On larger non-deuterated proteins with $\tau_c > 15$ ns, the sensitivity gain for methyl ^{13}C, ^{1}H correlations is 5–30%. It can be anticipated that it would be beneficial to utilize methyl ^{13}C, ^{1}H TROSY (Tugarinov et al. 2003) together with ^{15}N-HMQC for large ^{15}N, ^{2}H, ILV-methyl ^{13}C labeled proteins, but we did not test this approach here.

Conclusions

We have presented new NMR building blocks that can be utilized in experiments detecting simultaneously ^{15}N, ^{1}H and methyl ^{13}C, ^{1}H correlations. The pulse schemes provide theoretically optimal coherence transfer separately for IS spin system i.e., amide ^{15}N, ^{1}H correlations, and I_3S spin system i.e., methyl ^{13}C, ^{1}H correlations. The proposed pulse schemes were implemented in time-shared ^{15}N/$^{13}C_m$-HSQC and TROSY experiments and applied to three proteins. We observed significant sensitivity improvement with small proteins and to smaller extent even on 42 kDa MBP/β-Cyclodextrin complex. This suggests that time-shared ^{15}N/$^{13}C_m$-HSQC or TROSY pulse schemes can be used as building blocks for higher dimensionality NOESY experiments. The proposed methodology can also be very helpful for binding interface mapping by monitoring simultaneously perturbations in ^{15}N/^{1}H and methyl ^{13}C/^{1}H chemical shifts on uniformly ^{15}N and fractionally 10% ^{13}C labeled proteins, as demonstrated for the SH3 domain titrated with the target peptide. In this way, the sample typically used for stereo-specific assignment of diastereotopic methyl groups of leucines and valines can be utilized for binding studies.

Acknowledgments This work was financially supported by the grant 106852 (P. P.) from the Academy of Finland. P. W. is partly

supported by a fellowship from the National Graduate School in informational and structural biology of Finland.

References

Andersson P, Annila A, Otting G (1998) An α/β-HSQC-α/β experiment for spin-state selective editing of IS cross peaks. J Magn Reson 133:364–367

Bodenhausen G, Ruben J (1980) Natural abundance nitrogen-15 NMR by enhanced heteronuclear spectroscopy. Chem Phys Lett 69:185–189

Boelens R, Burgering M, Fogh RH, Kaptein R (1994) Time-saving methods for heteronuclear multidimensional NMR of (^{13}C, ^{15}N) doubly labeled proteins. J Biomol NMR 4:201–213

Farmer II, BT (1991) Simultaneous [^{13}C, ^{15}N]-HMQC, a pseudo-triple-resonance experiment. J Magn Reson 93:635–641

Farmer II, BT, Mueller L (1994) Simultaneous acquisition of [^{13}C, ^{15}N]- and [^{15}N, ^{15}N]-separated 4D gradient-enhanced NOESY spectra in proteins. J Biomol NMR 4:673–687

Frueh DP, Vosburg DA, Walsh CT, Wagner G (2006) Determination of all nOes in ^{1}H-^{13}C-Me-ILV-U-^{2}H-^{15}N proteins with two time-shared experiments. J Biomol NMR 34:31–40

Gardner KH, Konrat R, Rosen MK, Kay LE (1996) An (H)C(CO)NH-TOCSY pulse scheme for sequential assignment of protonated methyl groups in otherwise deuterated ^{15}N, ^{13}C-labeled proteins. J Biomol NMR 8:351–356

Geen H, Freeman R (1991) Band-selective radiofrequency pulses. J Magn Reson 93:93–141

Goto NK, Gardner KH, Mueller GA, Willis RC, Kay LE (1999) A robust and cost-effective method for the production of Val, Leu, Ile (delta 1) methyl-protonated ^{15}N-, ^{13}C-, ^{2}H-labeled proteins. J Biomol NMR 13:369–374

Grzesiek S, Bax A (1993) Amino acid type determination in the sequential assignment procedure of uniformly ^{13}C/^{15}N-enriched proteins. J Biomol NMR 3:185–204

Hajduk PJ, Augeri DJ, Mack J, Mendoza R, Yang J, Betz SF, Fesik SW (2000) NMR-based screening of proteins containing ^{13}C-labeled methyl groups. J Am Chem Soc 122:7898–7904

Iwai H, Fiaux J (2007) Use of biosynthetic fractional ^{13}C-labeling for backbone NMR assignment of proteins. J Biomol NMR 37: 187–193

Kay LE, Keifer P, Saarinen T (1992) Pure absorption gradient enhanced heteronuclear single quantum correlation spectroscopy with improved sensitivity. J Am Chem Soc 114:10663–10665

Kupče E, Boyd J, Campbell ID (1995) Short selective pulses for biochemical applications. J Magn Reson B 106:300–303

Kupče E, Wagner G (1995) Wideband homonuclear decoupling in protein spectra. J Magn Reson B 109:329–333

Marion D, Ikura M, Tschudin R, Bax A (1989) Rapid recording of 2D NMR spectra without phase cycling. Application to the study of hydrogen exchange in proteins. J Magn Reson 85:393–399

Neri D, Szyperski T, Otting G, Senn H, Wüthrich K (1989) Stereospecific nuclear magnetic resonance assignments of the methyl groups of valine and leucine in the DNA-binding domain of the 434 repressor by biosynthetically directed fractional ^{13}C labeling. Biochemistry 28:7510–7516

Nietlispach D (2005) Suppression of anti-TROSY lines in a sensitivity enhanced gradient selection TROSY scheme. J Biomol NMR 31:161–166

Nolis P, Parella T (2007) Simultaneous α/β spin-state selection for ^{13}C and ^{15}N from a time-shared HSQC-IPAP experiment. J Biomol NMR 37:65–77

Palmer AG, Cavanagh J, Wright PE, Rance M (1991) Sensitivity improvement in proton-detected two-dimensional heteronuclear correlation NMR spectroscopy. J Magn Reson 93:151–170

Pascal SM, Muhandiram DR, Yamazaki T, Forman-Kay JD, Kay LE (1994) Simultaneous acquisition of ^{15}N- and ^{13}C-edited NOE spectra of proteins dissolved in H_2O. J Magn Reson B103:197–201

Pervushin K, Riek R, Senn H, Wider G, Wüthrich K (1997) Attenuated T_2 relaxation by mutual cancellation of dipole-dipole coupling and chemical shift anisotropy indicates an avenue to NMR structures of very large biological macromolecules in solution. Proc Natl Acad Sci USA 94:12366–12371

Piotto M, Saudek V, Sklenář V (1992) Gradient-tailored excitation for single-quantum NMR spectroscopy of aqueous solutions. J Biomol NMR 2:661–665

Sattler M, Maurer M, Schleucher J, Griesinger C (1995) A simultaneous ^{15}N, ^{1}H- and ^{13}C, ^{1}H-HSQC with sensitivity enhancement and a heteronuclear gradient echo. J Biomol NMR 5:97–102

Schleucher J, Schwendinger M, Sattler M, Schmidt P, Schedletzky O, Glaser SJ, Sørensen OW, Griesinger C (1994) A general enhancement scheme in heteronuclear multidimensional NMR employing pulsed field gradients. J Biomol NMR 4:301–306

Senn H, Werner B, Messerle BA, Weber C, Traber R, Wüthrich K (1989) Stereospecific assignment of the methyl ^{1}H NMR lines of valine and leucine in polypeptides by nonrandom ^{13}C labelling. FEBS Lett 249:113–118

Shaka AJ, Barker PB, Freeman R (1985) Computer-optimized decoupling scheme for wideband applications and low-level operation. J Magn Reson 64:547–552

Sørensen OW (1990) Aspects and prospects of multidimensional time-domain spectroscopy. J Magn Reson 89:210–216

Tugarinov V, Hwang PM, Ollerenshaw JE, Kay LE (2003) Cross-correlated relaxation enhanced ^{1}H-^{13}C NMR spectroscopy of methyl groups in very high molecular weight proteins and protein complexes. J Am Chem Soc 125:10420–10428

Uhrín D, Bramham J, Winder SJ, Barlow P (2000) Simultaneous CT-^{13}C and VT-^{15}N chemical shift labelling: Application to 3D NOESY-CH_3NH and 3D ^{13}C,^{15}N HSQC-NOESY-CH_3NH. J Biomol NMR 18:253–259

Würtz P, Permi P (2007) SESAME-HSQC for simultaneous measurement of NH and CH scalar and residual dipolar couplings. Magn Reson Chem 45:289–295

Xia Y, Man D, Zhu G (2001) 3D Haro-NOESY-CH_3NH and Caro-NOESY-CH_3NH experiments for double labeled proteins. J Biomol NMR 19:355–360

Xia Y, Yee A, Arrowsmith CH, Gao X (2003) ^{1}HC and ^{1}HN total NOE correlations in a single 3D NMR experiment. ^{15}N and ^{13}C time-sharing in t1 and t2 dimensions for simultaneous data acquisition. J Biomol NMR, 193–203

Yang D, Kay LE (1999) Improved ^{1}HN-detected triple resonance TROSY-based experiments. J Biomol NMR 13:3–10

Supplementary

Goto NK, Kay LE (2000) New developments in isotope labeling strategies for protein solution NMR spectroscopy. Curr Opin Struct Biol 10:585–592

Hajduk PJ, Augeri DJ, Mack J, Mendoza R, Yang J, Betz SF, Fesik SW (2000) NMR-based screening of proteins containing ^{13}C-labeled methyl groups. J Am Chem Soc 122:7898–7904

Kay LE (2001) Nuclear magnetic resonance methods for high molecular weight proteins: a study involving a complex of maltose binding protein and beta-cyclodextrin. Methods Enzymol 339:174–203